

УДК 537.312:538.911'956

Doi: 10.31772/2712-8970-2024-25-1-157-166

**Для цитирования:** Магнитоемкость в сульфидах марганца с редкоземельным замещением  $Mn_{1-x}Re_xS$  / А. М. Харьков, О. Н. Бандурина, С. С. Аплеснин, Е. Г. Воронова // Сибирский аэрокосмический журнал. 2024. Т. 25, № 1. С. 157–166. Doi: 10.31772/2712-8970-2024-25-1-157-166.

**For citation:** Kharkov A. M., Bandurina O. N., Aplesnin S. S., Voronova E. G. [Magnetic capacity in manganese sulfides with rare earth substitution  $Mn_{1-x}Re_xS$ ]. *Siberian Aerospace Journal*. 2024, Vol. 25, No. 1, P. 157–166. Doi: 10.31772/2712-8970-2024-25-1-157-166.

---

## Магнитоемкость в сульфидах марганца с редкоземельным замещением $Mn_{1-x}Re_xS$

А. М. Харьков\*, О. Н. Бандурина, С. С. Аплеснин, Е. Г. Воронова

Сибирский государственный университет науки и технологий имени академика М. Ф. Решетнева  
Российская Федерация, 660037, г. Красноярск, просп. им. газ. «Красноярский рабочий», 31

\*E-mail: khark.anton@mail.ru

Исследуются поликристаллические образцы  $Mn_{1-x}Gd_xS$  и  $Mn_{1-x}Yb_xS$  с концентрацией  $x = 0,2$  вблизи концентрации протекания ионов по ГЦК решетки с целью определения флуктуации валентности иона иттербия на диэлектрические свойства. Диэлектрическая проницаемость и диэлектрические потери определены из измерения емкости и тангенса угла потерь в диапазоне частот  $10^2$ – $10^6$  Гц при температурах 80–500 К без магнитного поля и в магнитном поле. Магнитоемкость и диэлектрические потери в магнитном поле образца определялись из относительного изменения действительной и мнимой частей диэлектрической проницаемости образца в магнитном поле  $H = 12$  кЭ, приложенном параллельно обкладкам конденсатора. Обнаружен интервал температур с резким ростом диэлектрической проницаемости и максимумом диэлектрических потерь, который смещается с ростом частоты и магнитного поля. Найдено в  $Mn_{1-x}Yb_xS$  увеличение диэлектрической проницаемости и диэлектрических потерь в магнитном поле выше 170 К. Рост диэлектрических потерь объясняется увеличением времени релаксации в результате локальных деформаций вблизи ионов иттербия при флуктуациях валентности. Определен механизм уменьшения реактивного сопротивления в магнитном поле в  $Mn_{1-x}Yb_xS$  при низких частотах за счет емкости и при высоких частотах за счет индуктивности. В соединении  $Mn_{0,8}Gd_{0,2}S$  мнимая часть диэлектрической проницаемости имеет два максимума. Низкотемпературный максимум сдвигается в магнитном поле в сторону высоких температур и описывается в модели локализованных электронов с замерзанием дипольных моментов. Диэлектрические потери уменьшаются в магнитном поле. Магнитоемкость уменьшается на порядок в  $Mn_{0,8}Gd_{0,2}S$  по сравнению с  $Mn_{0,8}Yb_{0,2}S$ . Диэлектрическая проницаемость в обоих соединениях описывается в модели Дебая с активационной зависимостью времени релаксации от температуры, где энергии активации отличаются для ионов иттербия и гадолиния.

*Ключевые слова:* магнитоемкость, полупроводники, модель Дебая.

## Magnetic capacity in manganese sulfides with rare earth substitution $Mn_{1-x}Re_xS$

A. M. Kharkov\*, O. N. Bandurina, S. S. Aplesnin, E. G. Voronova

Reshetnev Siberian State University of Science and Technology  
31, Krasnoyarskii rabochii prospekt, Krasnoyarsk, 660037, Russian Federation

\*E-mail: khark.anton@mail.ru

*Polycrystalline samples  $Mn_{1-x}Gd_xS$  and  $Mn_{1-x}Yb_xS$  with a concentration  $x = 0.2$ , near the concentration of ion flow through the fcc lattice, are studied in order to determine fluctuations in the valence of the ytterbium ion on dielectric properties. Dielectric constant and dielectric losses were determined from measurements of capacitance and loss tangent in the frequency range  $10^2$ – $10^6$  Hz at temperatures of 80–500 K without a magnetic field and in a magnetic field. The magnetic capacity and dielectric losses in the magnetic field of the sample were determined from the relative change in the real and imaginary parts of the dielectric constant of the sample in a magnetic field  $H = 12$  kOe applied parallel to the capacitor plates. A temperature range with a sharp increase in dielectric constant and with a maximum dielectric loss has been discovered, which shifts with increasing frequency and magnetic field. An increase in dielectric constant and dielectric losses in a magnetic field above 170 K was found in  $Mn_{1-x}Yb_xS$ . The increase in dielectric losses is explained by an increase in relaxation time, as a result of local deformations near ytterbium ions during valence fluctuations. The mechanism for reducing reactance in a magnetic field in  $Mn_{1-x}Yb_xS$  at low frequencies due to capacitance, and at high frequencies due to inductance, has been determined. In the  $Mn_{0.8}Gd_{0.2}S$  compound, the imaginary part of the dielectric constant has two maxima. The low-temperature maximum shifts in a magnetic field towards high temperatures and is described in the model of localized electrons with freezing of dipole moments. Dielectric losses decrease in a magnetic field. The magnetic capacity decreases by an order of magnitude in  $Mn_{0.8}Gd_{0.2}S$  compared to  $Mn_{0.8}Yb_{0.2}S$ . The dielectric constant in both compounds is described in the Debye model with the activation dependence of the relaxation time on temperature, where the activation energies differ for ytterbium and gadolinium ions.*

*Keywords:* magnetic capacity, semiconductors, Debye model.

## Introduction

In spacecraft, electronics operate in extreme conditions with temperature differences of hundreds of degrees. It is necessary to find materials, for example, based on multiferroics, that can demonstrate stable operation under these conditions.

Materials, where the relationship between magnetic and electrical properties, magnetoelectrics and multiferroics is manifested, are of interest from both fundamental and applied points of view [1–4]. Specific attention is drawn to materials exhibiting magnetoelectric properties in the region of room and higher temperatures in connection with practical application in microelectronics for recording and storing information [5; 6]. Bismuth ferrite  $BiFeO_3$  belongs to such studied materials [7–9].  $LuFe_2O_4$  reveals the effect of giant magnetic capacity at room temperature and it is explained by charge fluctuations with different spin values in  $Fe^{2+}$  and  $Fe^{3+}$  ions as a result of the removal of degeneracy between the two types of charge order by an external magnetic field [10].

Magnetic capacity in an electrically inhomogeneous medium can be due to the Maxwell–Wagner effect [11–14] due to the tensor nature of the interaction of current carriers with the magnetic and electric fields and the mixing of longitudinal and transverse conductivity components. Within the model, the magnetic capacity is positive provided the size of the electrical inhomogeneity is an order of magnitude greater than the electron mean free path, the measurement time  $1/\omega$  exceeds the scattering time, and the matrix is dielectric [13].

Such effects clearly demonstrate that the presence of magnetic capacity is not sufficient to classify these compounds as multiferroics. On the other hand, magnetic capacitance without magnetoelectric coupling may be more practical for technological applications since the existence of long-range magnetic order is not required.

The dielectric constant and its response to a magnetic field depend on the degree of electrical inhomogeneity, which can be changed as a result of nonstoichiometric substitution in manganese sulfide, for example, by gadolinium ions with zero orbital magnetic moment and thulium, the orbital moment of which determines the electrical polarizability of the ion [15–19]. Besides, the ytterbium ion belongs to elements with variable valence [20–23], whose valence fluctuations will make an additional contribution to the dielectric constant and impedance [24–26].

The purpose of the study is to establish the effect of cation substitution on electrical polarization, the response of dielectric characteristics and dielectric losses to a magnetic field during electronic doping of semiconductors.

### X-ray diffraction analysis and methodology

The research focused on polycrystalline samples  $\text{Mn}_{1-x}\text{Gd}_x\text{S}$  and  $\text{Mn}_{1-x}\text{Yb}_x\text{S}$  with a concentration  $x = 0.2$ , near the concentration of ion flow through the fcc lattice. According to X-ray diffraction data, the samples have a fcc lattice type, similar to the original sulfide compounds [27]. Fig. 1 shows an X-ray diffraction pattern of the samples.

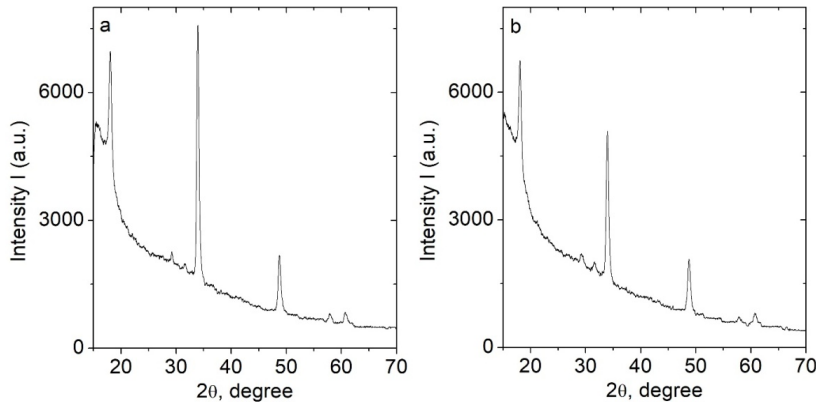


Рис. 1. Рентгеновская дифракционная картина образцов  $\text{Mn}_{0.85}\text{Yb}_{0.15}\text{S}$  (а) и  $\text{Mn}_{0.8}\text{Yb}_{0.2}\text{S}$  (б) при комнатной температуре

Fig. 1. X-ray diffraction pattern of  $\text{Mn}_{0.85}\text{Yb}_{0.15}\text{S}$  (a) and  $\text{Mn}_{0.8}\text{Yb}_{0.2}\text{S}$  (b) samples at room temperature

Gadolinium sulfide has a metallic type of conductivity, while ytterbium sulfide is a semiconductor with a gap in the electronic excitation spectrum. Under the influence of external pressure, the gap closes and YbS exhibits metallic properties. As the number of electrons increases, the unfilled  $4f$  levels move closer to the Fermi energy, which leads to a change in the electronic properties. The shift of the  $4f$  level to the Fermi energy occurs in heavy rare earth elements from GdS to YbS, where the  $4f$  level crosses the bottom of the band and is located in the forbidden gap [28–32].

Dielectric constant and dielectric losses are determined from capacitance and loss tangent measurements measured on an AM-3028 component analyzer in the frequency range  $10^2$ – $10^6$  Hz at temperatures of 80–500 K. Magnetic capacity  $\delta(\text{Re}(\varepsilon))$  and dielectric losses in the magnetic field of the sample were determined as

$$\delta(\text{Re}(\varepsilon)) = \frac{(\text{Re}(\varepsilon(H)) - \text{Re}(\varepsilon(0)))}{\text{Re}(\varepsilon(0))}; \quad \delta(\text{Im}(\varepsilon)) = \frac{(\text{Im}(\varepsilon(H)) - \text{Im}(\varepsilon(0)))}{\text{Im}(\varepsilon(0))}, \quad (1)$$

where  $\text{Re}(\varepsilon(H))$  and  $\text{Im}(\varepsilon(H))$  are the real and imaginary parts of the dielectric constant of the sample in a magnetic field  $H = 12$  kOe applied parallel to the capacitor plates, and  $\text{Re}(\varepsilon(0))$  is in a zero magnetic field. To prevent leakage currents, a layer of mica several micrometers thick was placed between the sample and the capacitor plates.

### Results and discussions

Fig. 2 shows the components of dielectric constant versus temperature for  $\text{Mn}_{0.8}\text{Yb}_{0.2}\text{S}$ . In the temperature range 160–180 K, the dielectric constant increases sharply, and the dielectric losses have a maximum, which shifts from  $T = 166$  K to  $T = 190$  K with an increase in frequency from 10 to 100 kHz. When heated, the dielectric constant in a magnetic field increases above 170 K (Fig. 2, b),

dielectric losses also increase several times. An increase in dielectric losses can be caused by an increase in relaxation time or an increase in conductivity in a magnetic field. Measuring the active and reactive components of impedance partially answers this question.

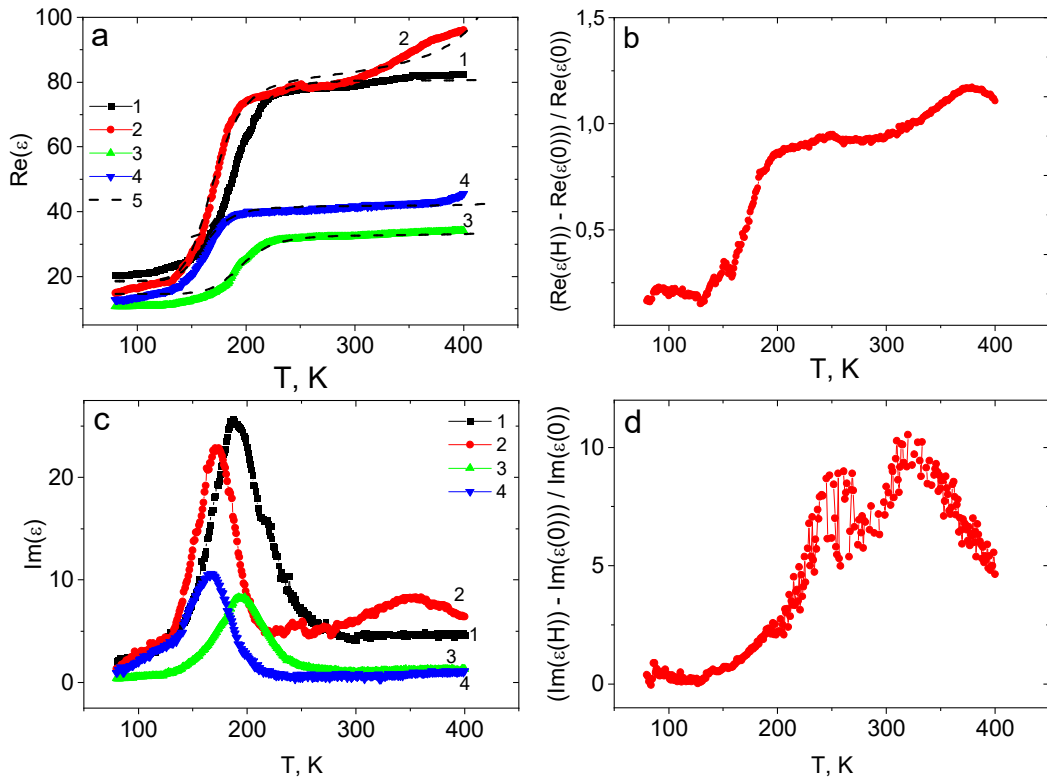


Рис. 2. Температурная зависимость действительной части диэлектрической проницаемости для образца  $\text{Mn}_{0.8}\text{Yb}_{0.2}\text{S}$ , измеренная в нулевом магнитном поле на частотах 100 кГц (3), 10 кГц (4) и в магнитном поле  $H = 8$  кЭ на частотах 100 кГц (1), 10 кГц (2). Теоретические расчеты в модели Дебая – пунктирные линии 5 (а). Относительное изменение действительной части диэлектрической проницаемости в магнитном поле  $H = 8$  кЭ на частоте 10 кГц (б). Температурная зависимость мнимой части диэлектрической проницаемости для образца  $\text{Mn}_{0.8}\text{Yb}_{0.2}\text{S}$ , измеренная в нулевом магнитном поле на частотах 100 кГц (3), 10 кГц (4) и в магнитном поле  $H = 8$  кЭ на частотах 100 кГц (1), 10 кГц (2) (в). Относительное изменение мнимой части диэлектрической проницаемости в магнитном поле  $H = 8$  кЭ на частоте 10 кГц (г).

Fig. 2. Temperature dependence of the real part of the dielectric constant for the  $\text{Mn}_{0.8}\text{Yb}_{0.2}\text{S}$  sample measured in a zero magnetic field at frequencies 100 kHz (3), 10 kHz (4) and in a magnetic field  $H = 8$  kOe at frequencies 100 kHz (1), 10 kHz (2). Theoretical calculations in the Debye model – dotted lines 5 (a). Relative change in the real part of the dielectric constant in a magnetic field  $H = 8$  kOe at frequency 10 kHz (b). Temperature dependence of the imaginary part of the dielectric constant for the  $\text{Mn}_{0.8}\text{Yb}_{0.2}\text{S}$  sample measured in a zero magnetic field at frequencies 100 kHz (3), 10 kHz (4) and in a magnetic field  $H = 8$  kOe at frequencies 100 kHz (1), 10 kHz (2) (c). Relative change in the imaginary part of the dielectric constant in a magnetic field  $H = 8$  kOe at frequency 10 kHz (d).

Fig. 3 shows the dependencies of resistance on alternating current and reactance without a magnetic field and in a magnetic field. The maximum resistance  $R(T)$  in a magnetic field shifts to the region of low temperatures. As a result, magnetoresistance in the temperature range 160–400 K changes sign and becomes negative. The reactance decreases by half at a frequency of 10 kHz in absolute value. The  $\text{Mn}_{0.8}\text{Yb}_{0.2}\text{S}$  compound has a high resistance and the reactance  $X = L\omega - 1/\omega C$  is mainly due to the capacitance. The decrease in  $X(H) / X(H = 0)$  is caused by an increase in capacitance, which is consistent with the magnetic capacity (Fig. 2, b).

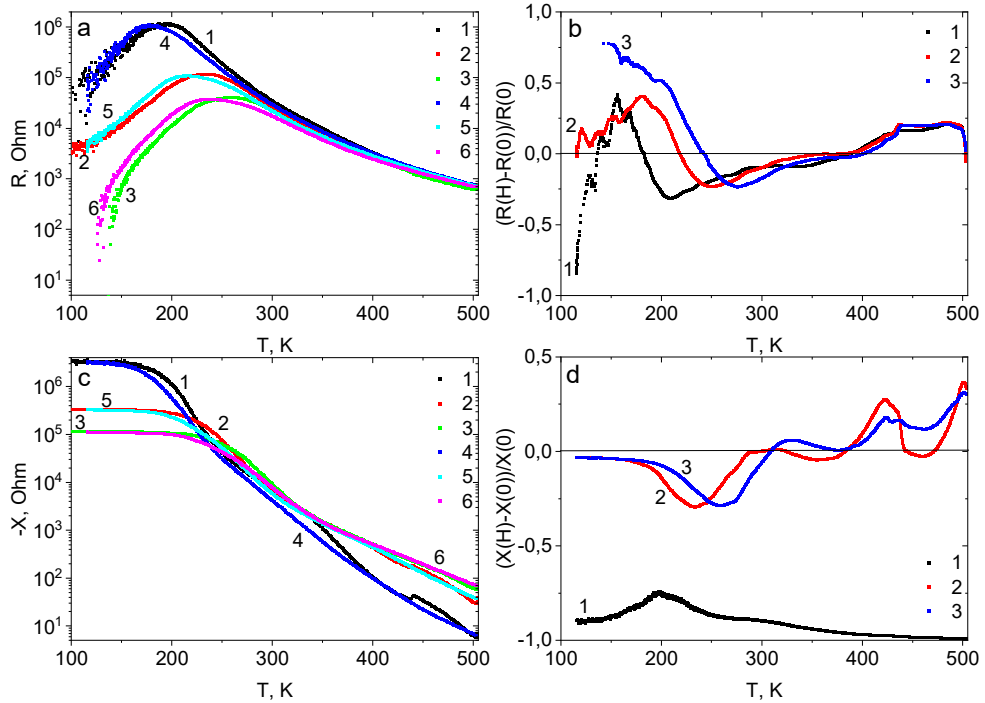


Рис. 3. Температурная зависимость активного сопротивления для образца  $\text{Mn}_{0.8}\text{Yb}_{0.2}\text{S}$  без поля (1, 2, 3) и в магнитном поле (4, 5, 6) на частотах 10 кГц (1, 4), 100 кГц (2, 5), 300 кГц (3, 6) (а). Магнитосопротивление активной части импеданса от температуры на частотах 10 кГц (1), 100 кГц (2), 300 кГц (3) (б). Зависимость реактивного сопротивления без поля (1, 2, 3) и в магнитном поле (4, 5, 6) на частотах 10 кГц (1, 4), 100 кГц (2, 5), 300 кГц (3, 6) (в). Магнитосопротивление реактивной части импеданса от температуры на частотах 10 кГц (1), 100 кГц (2), 300 кГц (3) (г)

Fig. 3. Temperature dependence of active resistance for the  $\text{Mn}_{0.8}\text{Yb}_{0.2}\text{S}$  sample without a field (1, 2, 3) and in a magnetic field (4, 5, 6) at frequencies 10 kHz (1, 4), 100 kHz (2, 5), 300 kHz (3, 6) (a). Magnetoresistance of the active part of the impedance versus temperature at frequencies 10 kHz (1), 100 kHz (2), 300 kHz (3) (b). Dependence of reactance on temperature without a field (1, 2, 3) and in a magnetic field (4, 5, 6) at frequencies 10 kHz (1, 4), 100 kHz (2, 5), 300 kHz (3, 6) (c). Magnetoresistance of the reactive part of the impedance versus temperature at frequencies 10 kHz (1), 100 kHz (2), 300 kHz (3) (d)

The qualitative difference between  $X(H)/X(H = 0)$  and  $C(H)/C(H = 0)$  at high frequencies  $\omega > 105$  Hz is due to the appearance of the inductive contribution of electrons in the vicinity of ytterbium ions. Electron hopping near an impurity center contributes to the appearance of an orbital magnetic moment and their synchronization in an external magnetic field. At low frequencies, a diffusion contribution is added, which is found from the impedance spectrum. In manganese sulfides substituted with elements of variable valence, large dielectric losses are observed due to local deformation near ytterbium ions during valence fluctuations. Dielectric losses are caused by electron-phonon interaction of current carriers with phonons. The imaginary part of the dielectric constant is related to the real part of the optical conductivity  $\sigma'$  by the relation  $\text{Im}(\epsilon) = \sigma'/\omega$ . In disordered semiconductors with hopping conductivity, a resonant and relaxation mechanism of conductivity can be realized.

Substitution of manganese with gadolinium does not qualitatively change the  $\epsilon(T)$  dependences presented in Fig. 4. The dielectric constant of  $\text{Mn}_{0.8}\text{Gd}_{0.2}\text{S}$  increases with heating and has an inflection at 170 K. The magnetic capacity decreases by an order of magnitude in  $\text{Mn}_{0.8}\text{Gd}_{0.2}\text{S}$  compared to  $\text{Mn}_{0.8}\text{Yb}_{0.2}\text{S}$ .

For the  $\text{Mn}_{0.8}\text{Gd}_{0.2}\text{S}$  composition, the dielectric constant is determined by localized electrons in the sublattice of manganese ions and conduction electrons in the gadolinium subsystem. The imaginary part of the dielectric constant  $\text{Im}(\epsilon(\omega))$ , shown in Fig. 5, has two maxima at  $T = 170$  K and  $T = 442$  K. The low-temperature maximum shifts in a magnetic field  $H = 8$  kOe towards high temperatures (Fig. 5).

Dielectric losses decrease in a magnetic field, except for the temperature range 194–279 K and 417–451 K (Fig. 5). We describe the low-temperature maximum in  $\text{Im}(\epsilon(\omega))$  at  $T = 170$  K in the model of localized electrons with freezing of dipole moments with activation energy  $\Delta E = 900$  K without a magnetic field and in a magnetic field  $\Delta E = 1050$  K.

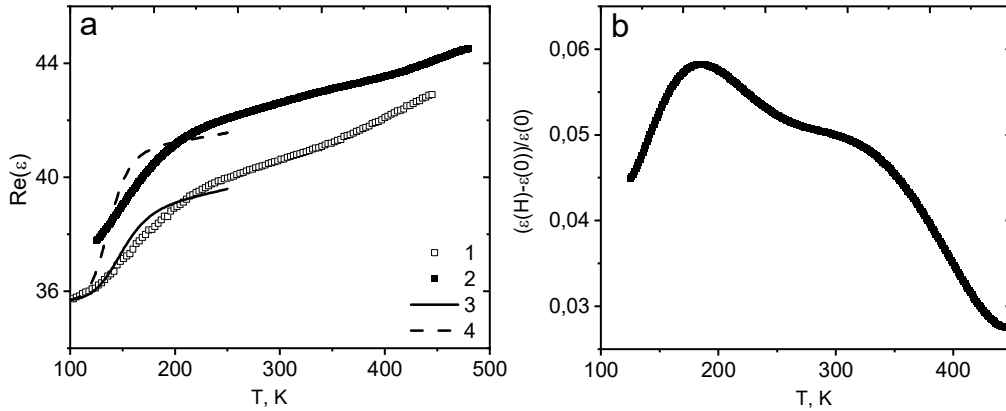


Рис. 4. Действительная часть диэлектрической проницаемости (а) от температуры для твердого раствора  $\text{Mn}_{0.8}\text{Gd}_{0.2}\text{S}$ , измеренная на частоте 10 кГц без поля (1) и в магнитном поле  $H = 8$  кЭ (2). Подгоночная функция  $\text{Re}(\epsilon) = A/(1 + B \exp(2\Delta E/T)) + \epsilon_0$  с энергией активации  $\Delta E = 900$  К (3),  $1050$  К (4) (а). Магнитоемкость в магнитном поле  $H = 8$  кЭ от температуры (б)

Fig. 4. Real part of the dielectric constant (a) on temperature for  $\text{Mn}_{0.8}\text{Gd}_{0.2}\text{S}$  solid solution, measured at a frequency of 10 kHz without a field (1) and in a magnetic field  $H = 8$  kOe (2). Fitting function  $\text{Re}(\epsilon) = A/(1 + B \exp(2\Delta E/T)) + \epsilon_0$  with activation energy  $\Delta E = 900$  K (3), 1050 K (4) (a). Magnetic capacity in a magnetic field  $H = 8$  kOe depending on temperature (b)

#### Fitting function

$$\text{Im}(\epsilon) = A_1 \cdot \exp(\Delta E / T) / (1 + B \cdot \exp(2\Delta E / T)); \quad \text{Re}(\epsilon) = \epsilon_0 + C / (1 + B \cdot \exp(2\Delta E / T)) \quad (2)$$

describes well the experimental data in Fig. 4 and 5 in the temperature range 100–250 K.

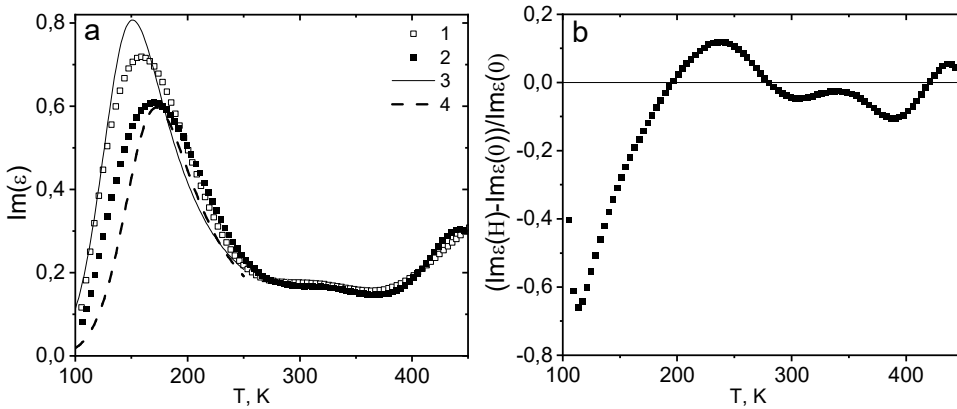


Рис. 5. Мнимая часть диэлектрической проницаемости (а) от температуры для твердого раствора  $\text{Mn}_{0.8}\text{Gd}_{0.2}\text{S}$ , измеренная на частоте 10 кГц без поля (1) и в магнитном поле  $H = 8$  кЭ (2). Подгоночная функция с энергией активации 900 К (3), 1050 К (4) (а). Относительное изменение мнимой части диэлектрической проницаемости в магнитном поле от температуры (б)

Fig. 5. Imaginary part of the dielectric constant (a) on temperature for  $\text{Mn}_{0.8}\text{Gd}_{0.2}\text{S}$  solid solution, measured at a frequency of 10 kHz without a field (1) and in a magnetic field  $H = 8$  kOe (2). Fitting function with activation energy 900 K (3), 1050 K (4) (a). Relative change in the imaginary part of the dielectric constant in a magnetic field on temperature (b)

The maximum decrease in dielectric losses in a magnetic field was observed in the vicinity of the Néel temperature and was caused by a decrease in the scattering of charged particles on spin fluctuations, which were suppressed by the magnetic field. The increase in dielectric constant above room temperature was caused by an increase in the electron delocalization radius and the disappearance of orbital-charge ordering.

The dielectric constant of  $\text{Mn}_{0.8}\text{Yb}_{0.2}\text{S}$  is described by formula (2) in the Debye model with the activation dependence of the relaxation time  $\tau_c = \tau_0 \cdot \exp(\Delta E / kT)$ , where  $\Delta E$  is the activation energy ( $\Delta E = 0.17 \text{ eV}$ ).

### Conclusion

The replacement of manganese ions by rare earth ions in the flow region results in a significant difference in dielectric properties. The presence of ions of variable valence leads to an increase in dielectric constant by a factor of two and dielectric losses by an order of magnitude compared to  $\text{Mn}_{0.8}\text{Gd}_{0.2}\text{S}$ . This is caused by valence fluctuation and strong electron-lattice coupling. Upon transition to the antiferromagnetic state, dielectric losses decrease by half in a magnetic field in  $\text{Mn}_{0.8}\text{Gd}_{0.2}\text{S}$  and do not change in  $\text{Mn}_{0.8}\text{Yb}_{0.2}\text{S}$ . Above room temperature, the imaginary part of the dielectric constant increases by an order of magnitude in  $\text{Mn}_{0.8}\text{Yb}_{0.2}\text{S}$ . The decrease in reactance in  $\text{Mn}_{0.8}\text{Yb}_{0.2}\text{S}$  in a magnetic field at low frequencies is caused by an increase in capacitance, and at high frequencies it happens due to an increase in inductance.

### Библиографические ссылки

1. Khomskii D. Classifying multiferroics: Mechanisms and effects // Physics 2009. Vol. 2. P. 20.
2. High Energy Storage Properties and Electrical Field Stability of Energy Efficiency of  $(\text{Pb}_{0.89}\text{La}_{0.11})(\text{Zr}_{0.70}\text{Ti}_{0.30})_{0.9725}\text{O}_3$  Relaxor Ferroelectric Ceramics / A. Kumar, S. H. Kim, M. Peddigari et al. // Electron. Mater. Lett. 2019. Vol. 15. P. 323–330.
3. Mostovoy M. V. Ferroelectricity in Spiral Magnets // Phys. Rev. Lett. 2006. Vol. 96. P. 067601.
4. Progress in multiferroic and magnetoelectric materials: applications, opportunities and challenges / M. Kumar, S. Shankar, A. Kumar, et. al. // J. Mater. Sci.: Mater. Electron. 2020. Vol. 31. P. 19487–19510.
5. Eerenstein W., Mathur N. D., Scott J. F. Multiferroic and magnetoelectric materials // Nature. 2006. Vol. 442. P. 759.
6. Ederer C., Spaldin N. A. Weak ferromagnetism and magnetoelectric coupling in bismuth ferrite // Phys. Rev. B. 2005. Vol. 71. P. 060401.
7. Epitaxial  $\text{BiFeO}_3$  multiferroic thin film heterostructures / J. Wang, J. B. Neaton, H. Zheng et al. // Science. 2003. Vol. 299. P. 1719.
8. Пятаков А. П., Звездин А. К. Магнитоэлектрические материалы и мультиферроиды // УФН. 2012. Т. 182. С. 593–620.
9. Structural and Magnetic Transitions in the  $\text{Bi}_2\text{Fe}_4\text{O}_9/\text{BiFeO}_3$  Composite / L. V. Udod, S. S. Aplesnin, M. N. Sitnikov et al. // J. All. Comp. 2023. Vol. 957, No 2. P. 170445.
10. Magnetoelectric Effect Driven by Magnetic Domain Modification in  $\text{LuFe}_2\text{O}_4$  / T. Kambe, Y. Fukada, J. Kano et al. // Phys. Rev. Lett. 2013. Vol. 110. P. 117602.
11. Maxwell J. C. Treatise on Electricity and Magnetism. 3rd ed. Dover. New York. 1991. P. 5–531.
12. Апленчин С. С., Ситников М. Н., Живулько А. М. Смена знака магнитоемкости в парамагнитной области в катион-замещенном селениде марганца // ФТТ. 2018. Т. 60, Вып. 4. С. 670–676.
13. Parish M. M., Littlewood P. B. Magnetocapacitance in Nonmagnetic Composite Media // Phys. Rev. Lett. 2008. Vol. 101. P. 166602.
14. Effect of the Electrical Inhomogeneity on the Magnetocapacitance Sign Change in the  $\text{Ho}_x\text{Mn}_{1-x}\text{S}$  Semiconductors upon Temperature and Frequency Variation / S. S. Aplesnin, M. N. Sitnikov, A. M. Kharkov, H. Abdelbaki // J. Mater. Sci.: Mater. Electron. 2023. Vol. 34. P. 284.

15. Aplesnin S. S., Kharkov A. M., Filipson G. Yu. Magnetic capacitance in variable-valence manganese sulfides // Phys. Stat. Sol. B. 2020. Vol. 257, No. 5. P. 1900637.
16. Апленчин С. С., Ситников М. Н. Магнитотранспортные эффекты в парамагнитном состоянии в  $Gd_xMn_{1-x}S$  // Письма в ЖЭТФ. 2014. Т. 100? Вып. 2. С. 104–110.
17. Апленчин С. С., Ситников М. Н. Магнитоемкостный эффект в  $Gd_xMn_{1-x}S$  // ФТТ. 2016. Т. 58, Вып. 6. С. 1112.
18. Influence of induced electrical polarization on the magnetoresistance and magnetoimpedance in the spin-disordered  $Tm_xMn_{1-x}S$  solid solution / S. S. Aplesnin, M. N. Sitnikov, A. M. Kharkov et al. // Phys. Stat. Sol. B. 2019. Vol. 256. P. 1900043.
19. Magnetocapacity of manganese sulphides substituted by thulium ions / A. M. Kharkov, M. N. Sitnikov et al. // IOP Conf. Ser.: Mater. Sci. Eng. 2020. Vol. 822. P. 012024.
20. Handbook on the Physics and Chemistry of Rare Earths / P. Wachter // Phys. Rev. B. 1989. P. 132.
21. Optical response of YbS and YbO at high pressures and pressure-volume relation of YbS / K. Syassen, H. Winzen, H. G. Zimmer et al. // Phys. Rev. B. 1985. Vol. 32. P. 8246.
22. Photoemission Evidence for Valence Fluctuations and Kondo Resonance in  $YbAl_2$  / M. Matsunami, A. Chainani, M. Taguchi et al. // Phys. Rev. B. 2008. Vol. 78. P. 195118.
23. Pressure Tuning of an Ionic Insulator into a Heavy Electron Metal: An Infrared Study of YbS // M. Matsunami, H. Okamura, A. Ochiai, T. Nanba // Phys. Rev. Lett. 2009. Vol. 103. P. 237202.
24. Spin state of cations and magnetoelastic effect in the  $Mn_{1-x}Yb_xS$  / S. S. Aplesnin, A. M. Kharkov, O. B. Romanova et al. // JMMM. 2014. Vol. 352. P. 1–5.
25. Magnetoimpedance, Jahn-Teller transitions upon electron doping of manganese sulfide / S. S. Aplesnin, M. N. Sitnikov, A. M. Kharkov et al. // JMMM. 2020. Vol. 513. P. 167104.
26. Aplesnin S. S., Kharkov A. M., Sokolov V. V. Gigantic magnetocapacitive effect into  $Yb_xMn_{1-x}S$  // Abstracts. V Euro-Asian Symposium «Trends in Magnetism»: Nanospintronics Eastmag, Vladivostok. 2013. С. 33–34.
27. Spin-dependent transport in  $\alpha$ -MnS single crystals / S. S. Aplesnin, L. I. Ryabinkina, G. M. Abramova et al. // Phys. Sol. St. 2004. Vol. 46, Is. 11. P. 2067.
28. Understanding the valency of rare earths from first-principles theory / P. Strange, A. Svane, W. M. Temmerman et al. // Nature 1999. Vol. 399. P. 756.
29. Simple rules for determining valencies of f-electron systems / L. Petit, A. Svane, Z. Szotek et al. // J. Phys.: Cond. Mat. 2001. Vol. 13. P. 8697–8706.
30. Aplesnin S. S., Romanova O. B., Yanushkevich K. I. Magnetoresistance effect in anion-substituted manganese chalcogenides // Phys. Stat. Sol. B.: Basic Research 2015. Vol. 252, Is. 8. P. 1792.
31. Universal scaling in the dynamical conductivity of heavy fermion Ce and Yb compounds / H. Okamura, T. Watanabe, M. Matsunami et al. // J. Phys. Soc. Jpn. 2007. Vol. 76. P. 023703.
32. Annese E. Definitive Evidence for Fully Occupied 4f Electrons in YbS and Yb Metal // Phys. Rev. B. 2004. Vol. 70. P. 075117.

## References

1. Khomskii D. Classifying multiferroics: Mechanisms and effects. *Physics*. 2009, Vol. 2, P. 20.
2. Kumar A., Kim S. H., Peddigari M. et al. High Energy Storage Properties and Electrical Field Stability of Energy Efficiency of  $(Pb_{0.89}La_{0.11})(Zr_{0.70}Ti_{0.30})_{0.9725}O_3$  Relaxor Ferroelectric Ceramics. *Electron. Mater. Lett.* 2019, Vol. 15, P. 323–330.
3. Mostovoy M. V. Ferroelectricity in Spiral Magnets. *Phys. Rev. Lett.* 2006, Vol. 96, P. 067601.
4. Kumar M., Shankar S., Kumar A. et al. Progress in multiferroic and magnetoelectric materials: applications, opportunities and challenges. *J. Mater. Sci.: Mater. Electron.* 2020, Vol. 31, P. 19487–19510.

5. Eerenstein W., Mathur N. D., Scott J. F. Multiferroic and magnetoelectric materials. *Nature*. 2006, Vol. 442, P. 759.
6. Ederer C., Spaldin N. A. Weak ferromagnetism and magnetoelectric coupling in bismuth ferrite. *Phys. Rev. B*. 2005, Vol. 71, P. 060401.
7. Wang J., Neaton J.B., Zheng H. Epitaxial  $\text{BiFeO}_3$  multiferroic thin film heterostructures. *Science*. 2003, Vol. 299, P. 1719.
8. Pyatakov A. P., Zvezdin A. K. [Magnetoelectric materials and multiferroics]. *UFN*. 2012, Vol. 182, P. 593–620 (In Russ.).
9. Uddod L. V., Aplesnin S. S., Sitnikov M. N. et al. Structural and Magnetic Transitions in the  $\text{Bi}_2\text{Fe}_4\text{O}_9/\text{BiFeO}_3$  Composite. *J. All. Comp.* 2023, Vol. 957, No 2, P. 170445.
10. Kambe T., Fukada Y., Kano J. et al. Magnetoelectric Effect Driven by Magnetic Domain Modification in  $\text{LuFe}_2\text{O}_4$ . *Phys. Rev. Lett.* 2013, Vol. 110, P. 117602.
11. Maxwell J. C. Treatise on Electricity and Magnetism. 3rd ed., Dover, New York, 1991, P. 5–531.
12. Aplesnin S. S., Sitnikov M. N., Zhivulko A. M. [Change of sign of magnetic capacity in the paramagnetic region in cation-substituted manganese selenide]. *FTT*. 2018, Vol. 60, Is. 4, P. 670–676 (In Russ.).
13. Parish M. M., Littlewood P. B. Magnetocapacitance in Nonmagnetic Composite Media. *Phys. Rev. Lett.* 2008, Vol. 101, P. 166602.
14. Aplesnin S. S., Sitnikov M. N., Kharkov A. M., Abdelbaki H. Effect of the Electrical Inhomogeneity on the Magnetocapacitance Sign Change in the  $\text{Ho}_x\text{Mn}_{1-x}\text{S}$  Semiconductors upon Temperature and Frequency Variation. *J. Mater. Sci.: Mater. Electron.* 2023, Vol. 34, P. 284.
15. Aplesnin S. S., Kharkov A. M., Filipson G. Yu. Magnetic capacitance in variable-valence manganese sulfides. *Phys. Stat. Sol. B*. 2020, Vol. 257, No. 5, P. 1900637.
16. Aplesnin S. S., Sitnikov M. N. [Magnetotransport effects in the paramagnetic state in  $\text{Gd}_x\text{Mn}_{1-x}\text{S}$ ]. *Letters to JETP*. 2014, Vol. 100, Is. 2, P. 104–110 (In Russ.).
17. Aplesnin S. S., Sitnikov M. N. [Magnetic capacitance effect in  $\text{Gd}_x\text{Mn}_{1-x}\text{S}$ ]. *FTT*. 2016, Vol. 58, Is. 6, P. 1112 (In Russ.).
18. Aplesnin S. S., Sitnikov M. N., Kharkov A. M., Masyugin A. N., Kretinin V. V., Fisenko O. B., Gorev M. V. Influence of induced electrical polarization on the magnetoresistance and magnetoimpedance in the spin-disordered  $\text{Tm}_x\text{Mn}_{1-x}\text{S}$  solid solution. *Phys. Status Solidi B*. 2019, Vol. 256, P. 1900043.
19. Kharkov A. M., Sitnikov M. N. et al. Magnetocapacity of manganese sulphides substituted by thulium ions. *IOP Conf. Ser.: Mater. Sci. Eng.* 2020, Vol. 822, P. 012024.
20. Wachter P. Handbook on the Physics and Chemistry of Rare Earths. *Phys. Rev. B*. 1989, P. 132.
21. Syassen K., Winzen H., Zimmer H. G. et al. Optical response of  $\text{YbS}$  and  $\text{YbO}$  at high pressures and pressure-volume relation of  $\text{YbS}$ . *Phys. Rev. B*. 1985, Vol. 32, P. 8246.
22. Matsunami M., Chainani A., Taguchi M. et al. Photoemission Evidence for Valence Fluctuations and Kondo Resonance in  $\text{YbAl}_2$ . *Phys. Rev. B*. 2008, Vol. 78, P. 195118.
23. Matsunami M., Okamura H., Ochiai A., Nanba T. Pressure Tuning of an Ionic Insulator into a Heavy Electron Metal: An Infrared Study of  $\text{YbS}$ . *Phys. Rev. Lett.* 2009, Vol. 103, P. 237202.
24. Aplesnin S. S., Kharkov A. M., Romanova O. B. et al. Spin state of cations and magnetoelastic effect in the  $\text{Mn}_{1-x}\text{Yb}_x\text{S}$ . *JMMM*. 2014, Vol. 352, P. 1–5.
25. Aplesnin S. S., Sitnikov M. N., Kharkov A. M. et al. Magnetoimpedance, Jahn-Teller transitions upon electron doping of manganese sulfide. *JMMM*. 2020, Vol. 513, P. 167104.
26. Aplesnin S. S., Kharkov A. M., Sokolov V. V. Gigantic magnetocapacitive effect into  $\text{Yb}_x\text{Mn}_{1-x}\text{S}$ . Abstracts. V Euro-Asian Symposium Trends in Magnetism: Nanospintrronics Eastmag, Vladivostok, 2013, P. 33–34.
27. Aplesnin S. S., Ryabinkina L. I., Abramova G. M. Spin-dependent transport in  $\alpha$ - $\text{MnS}$  single crystals. *Phys. Sol. St.* 2004, Vol. 46, Is. 11, P. 2067.

28. Strange P., Svane A., Temmerman W. M. et al. Understanding the valency of rare earths from first-principles theory. *Nature*. 1999, Vol. 399, P. 756.
29. Petit L., Svane A., Szotek Z. et al. Simple rules for determining valencies of f-electron systems. *J. Phys.: Cond. Mat.* 2001, Vol. 13, P. 8697–8706.
30. Aplesnin S. S., Romanova O. B., Yanushkevich K. I. Magnetoresistance effect in anion-substituted manganese chalcogenides. *Phys. Stat. Sol. B.: Basic Research*. 2015, Vol. 252, Is. 8, P. 1792.
31. Okamura H., Watanabe T., Matsunami M. et al. Universal scaling in the dynamical conductivity of heavy fermion Ce and Yb compounds. *J. Phys. Soc. Jpn.* 2007, Vol. 76, P. 023703.
32. Annese E. Definitive Evidence for Fully Occupied 4f Electrons in YbS and Yb Metal. *Phys. Rev. B*. 2004, Vol. 70, P. 075117.

© Харьков А. М., Бандурина О. Н., Аплеснин С. С., Воронова Е. Г., 2024

---

**Харьков Антон Михайлович** – кандидат физико-математических наук, доцент кафедры физики; Сибирский государственный университет науки и технологий имени академика М. Ф. Решетнева. E-mail: kharkanton@mail.ru.

**Бандурина Ольга Николаевна** – кандидат физико-математических наук, доцент кафедры физики; Сибирский государственный университет науки и технологий имени академика М. Ф. Решетнева. E-mail: bandurinaon@yandex.ru.

**Аплеснин Сергей Степанович** – доктор физико-математических наук, заведующий кафедрой физики; Сибирский государственный университет науки и технологий имени академика М. Ф. Решетнева. E-mail: aplesnin@sibsau.ru.

**Воронова Евгения Григорьевна** – аспирант, институт космической техники; Сибирский государственный университет науки и технологий имени академика М. Ф. Решетнева. E-mail: evg.danilenko@mail.ru.

**Kharkov Anton Mikhailovich** – Cand. Sc., Associate Professor of the Department of Physics; Reshetnev Siberian State University of Science and Technology. E-mail: kharkanton@mail.ru.

**Bandurina Olga Nikolaevna** – Cand. Sc., Associate Professor of the Department of Physics; Reshetnev Siberian State University of Science and Technology. E-mail: bandurinaon@yandex.ru.

**Aplesnin Sergey Stepanovich** – Dr. Sc., Professor of the Department of Physics; Reshetnev Siberian State University of Science and Technology. E-mail: aplesnin@sibsau.ru.

**Voronova Evgenia Grigorievna** – post-graduate student, Institute of Space Technology; Reshetnev Siberian State University of Science and Technology. E-mail: evg.danilenko@mail.ru.

---